Preprints (www.preprints.org) | NOT PEER-REVIEWED | Posted: 14 June 2021 doi:10.20944/preprints202106.0369.v1

Dendrogramic representation of data: CHSH-violation vs. nonergodicity

[2,3]**Shor, Oded**;[1,2,3] **Benninger, Felix**; [4]**Khrennikov, Andrei**,

[1]Department of Neurology, Rabin Medical Center, Petach Tikva, Israel; [2]Felsenstein Medical Research Center, Beilinson Hospital, Petach Tikva, Israel; [3]Sackler Faculty of Medicine, Tel Aviv University, Tel Aviv, Israel; [4]Faculty of Technology, Department of Mathematics Linnaeus University, Växjö, Sweden.

Abstract: This paper is devoted to the foundational problems of *dendrogramic holographic theory* (DH-theory). We use the ontic-epistemic (implicate-explicate order) methodology. The epistemic counterpart is based on representation of data by dendrograms constructed with hierarchic clustering algorithms. The ontic Universe is described as the p-adic tree; it is zero dimensional, totally disconnected, disordered, and bounded (in p-adic ultrametric). Interrelation classical-quantum loses its sharpness; generally simple dendrograms are ``more quantum'' than complex one. We use the CHSH-inequality as a measure of quantum(-likeness). We demonstrate that it can be violated by classical experimental data represented by dendrograms. The seed of this violation is neither nonlocality nor rejection of realism. This is nonergodicity of dendrogramic time series. Generally, violation of ergodicity is one of the basic features of DH-theory. We also consider DH-theory for Minkovski geometry and monitor the dependence of CHSH-violation and nonergodicity on geometry as well as a Lorentz transformation of data.

Introduction

A model for the Universe based on the hierarchic relational representation of its components was suggested in [1]. The present paper is devoted to the foundational problems structured within Primas-

© 2021 by the author(s). Distributed under a Creative Commons CC BY license.

Preprints (www.preprints.org) | NOT PEER-REVIEWED | Posted: 14 June 2021 doi:10.20944/preprints202106.0369.v1

Atmanspacher [2,3] ontic-epistemic and Herz-Boltzmann [4,5] descriptive-observational structuring of physical theories (see also [6,7,8]), as well as Bohm's [9] implicate-explicate order viewpoint on the Universe. One of the aims of our study is re-establishing of realism in physics (cf. [10]-[18]).

We also describe representation of experimental data by dendrograms using *hierarchic clustering algorithms*. It leads to the p-adic model at the ontic level. (From this viewpoint, our research is a part of p-adic theoretical physics, see, e.g., [19]-[28], see section 6.) In [1], we named our theory *dendrogramic holographic theory* (DH-theory). In this paper, we shall not discuss holography (see [1]) but proceed with the same name.

The p-adic tree (*p> 1* is a natural number) is the infinite tree with the homogeneous structure of branching at each node, one incoming and p outcoming edges. This tree is endowed with natural metric (so-called ultrametric) and the algebraic structure of a ring (see appendix A).

We recall that an ontic theory is about reality as it is and the epistemic one is about knowledge collected through observations. The ontic Universe is unapproachable by observers. Nevertheless, its structure can be theoretically reconstructed by increasing the size of dendrograms; observer *O* generates approximations of the ontic Universe. The limiting mathematical structure is uniquely determined -- the *p*-adic tree (or algebraically a ring denoted as **Zp*)*.

One of the main aims of novel mathematical modelling of ontic-epistemic structuring is better understanding of the classical-quantum interrelation. We recall that *quantum mechanics is an epistemic model*, it is about observations' outcomes (see Bohr [29,30] and Plotnitsky [31-33). In DH-theory, ``quantumness" is present only at the level of dendrograms, and the p-adic ontic Universe is classical. The heuristic criterium of quantum-likeness is very natural: simple dendrograms are more quantum(-like) than complex dendrograms. As a test of quantum-likeness, we use the *CHSH-inequality*, not for the standard observables, but for new observables reflecting the hierarchic relational structure of data. It should be highlighted that the original experimental data used in

Preprints (www.preprints.org) | NOT PEER-REVIEWED | Posted: 14 June 2021 doi:10.20944/preprints202106.0369.v1

this paper is classical. Its quantum-like structure becomes visible through dendrogramic representation. The seed of the violation of the CHSH-inequality is neither nonlocality nor rejection of realism. This is *nonergodicity* of dendrogramic time series. This is the good place to recall that a few authors had coupled quantum behaviour with violation of ergodicity [34-38]. We also consider DH-theory for Minkovski geometry and monitor the dependence of CHSH-violation and nonergodicity on geometry as well as a Lorentz transformation of data.

The reader who is not interested in foundations can jump directly to section 7 devoted to experimental data, correlations, and violation of the CHSH-inequality for hierarchic observables and its correlation of nonergodicity of data.

2. Dendrogram representation of the Universe

2.1. Systems as clusters of clicks of detectors

By Bohr the outcomes of measurements are not the objective properties of systems [29-33]. They quantitively represent interrelation between a system S and an observer O. An ontic system exists independently of O. However, it is unapproachable by the observer; in fact, O constructs its approximate representation by using data.

Consider an observer O constructing representation of surrounding environment, in the extreme case, of the Universe. In DH-theory, the observer has the free choice not only to perform or not perform some observation, but even the free choice for decomposition of collected data into blocks and treating these blocks as (epistemic) systems' representation. *The fundamental entities of the epistemic theory are events* (cf. [14, 39-43]), *not systems.* Systems are determined as clusters of events – say clicks of detectors (or other detection events). This position is very close to the view of Zeilinger on quantum mechanics (private discussions of with Akh).

Preprints (www.preprints.org) | NOT PEER-REVIEWED | Posted: 14 June 2021 doi:10.20944/preprints202106.0369.v1

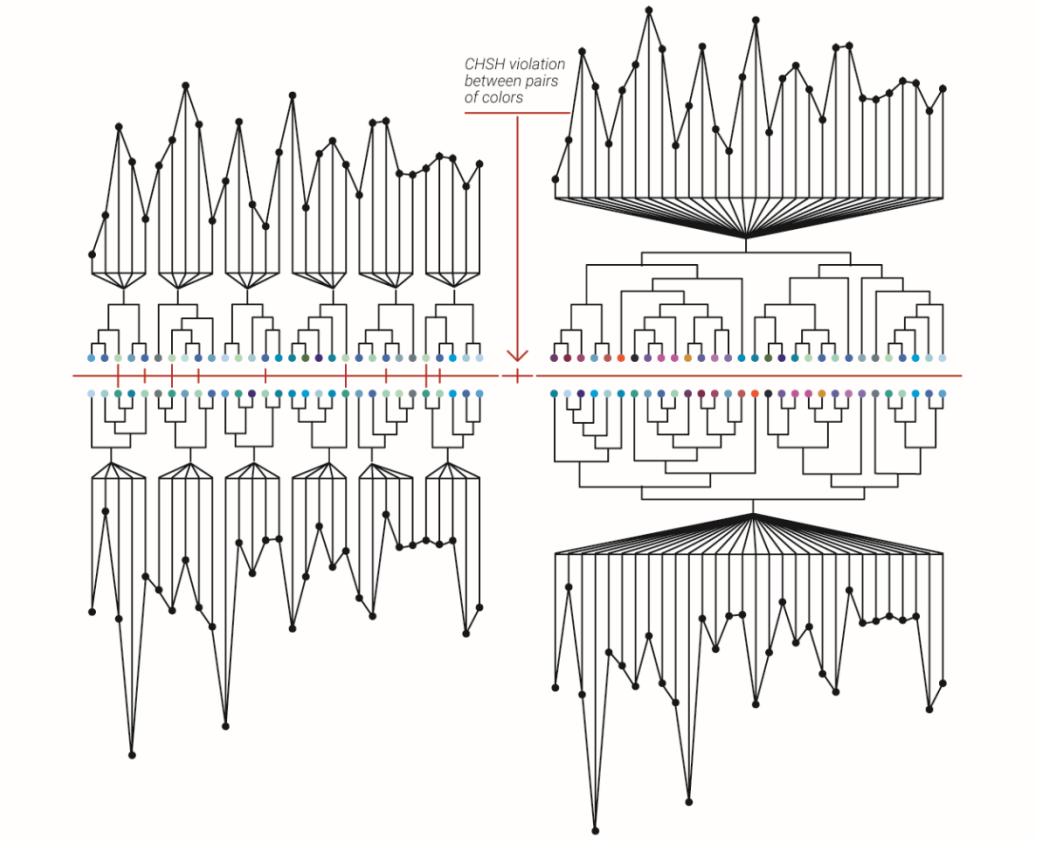

illustration 1. Dendrogramic representation of two time series (graphs) by dendrograms, LHS: d=5, RHS: d= 30.

2.2. Representation of systems by dendrograms

Simple collection of experimental statistical data does not tell observer *O* about the *genuine hierarchic* interrelations between physical processes under observations. Such hierarchic structure which can be approximately recovered with the aid of *clustering algorithms.* This hierarchic clustering leads to the treelike geometry. In DH-theory, (epistemic) systems are described by *dendrograms,* finite trees. Any observer *O* can reconstruct his environment and, in the limit, the whole *O*-Universe by collecting observational data.

Preprints (www.preprints.org) | NOT PEER-REVIEWED | Posted: 14 June 2021 doi:10.20944/preprints202106.0369.v1

In DH-thery, *decomposition of the O-Universe into subsystems is done through decomposition of data into blocks*. Each block of data is represented by dendrogram -- this is a system. The data can be subdivided into blocks in different ways. The *O*-Universe can be decomposed into systems of different complexity depending on blocks' size. We illustrate this process on Fig. 1a by dividing data into the blocks of the equal size, d=5, LHS, and Fig1 b, d=30.

2.3. P-adic metric for hierarchic relations

The points at the baselevel of any dendrogram *D* (see Fig.1) represent the relational characteristics of the system expressed by *D*. For the simplest hierarchic algorithms, based on choices of just two alternatives – two branching at vertexes, the basepoints can be described by vectors with coordinates 0/1. The natural distance between these characteristics is given by 2-adic ultrametric *r_2*: longer the common root of the paths going from the dendrogram's root to points *a, b* – shorter the distance between them (see appendix A). This metric encodes the hierarchic relations inside the dendrogramic system and with its surrounding environment. More general hierarchic clustering algorithms with *p*-branching at vertexes generate representation of systems by dendrograms having more complex topology. (Here p>1 is a natural number determining the tree structure). The branches (and the corresponding end-points) are encoded by vectors with the coordinates belonging to the set{0,1,...,p-1}. The corresponding common root distance is denoted by *r_p.*

Take two points *a, b* at the baselevel of dendrogram *D* representing a system, the common root distance *r_p(a,b)* gives the quantification of closeness of these two system's characteristics w.r.t. the hierarchic order relation. The quantity

$$R\_D = max\{ r\_p(a,b): a, b \text{ belong to } D\}$$

(dendrogram's diameter) determines the degree of hierarchic interrelation between the elements of the dendrogram-system. If *R_D* is small the system's characteristics are highly relationally connected, if *R_D* is large, the system is relationally sparse.

Preprints (www.preprints.org) | NOT PEER-REVIEWED | Posted: 14 June 2021 doi:10.20944/preprints202106.0369.v1

2.4. Epistemic realism, hidden variables

Each dendrogram *D* can be represented by the vectors with coordinates belonging to the set {0,1,...,p-1}. These are (hierarchic relational) *hidden variables*. Observer can invent relational observables defined as functions of these hidden variables: A=A(u). This is *the realistic model of observations* which is constructed by the observer *O* through hierarchic structuring of the experimental data. This approach can be called *realism without reality*, as opposite to *reality without realism* viewpoint on quantum physics suggested by Plotnitsky [33, 44]. Such hidden variables are constructed on the basis of experimental data, they are so to say epistemic variables. But the mathematical model is realistic in the sense of set-theoretical representation of states - hidden variables and observables - functions of these variables.

3. From epistemic (explicate) to ontic (implicate): p-adic Universe.

By considering the data blocks of increasing size, in the limit *O* can reconstruct the ontic description. The dendrogram based epistemic theory leads to the p-adic geometry of the ontic Universe. (The role of the model parameter p will be discussed in section 5.) In the limit, dendrograms of increasing size generate the infinite p-adic tree endowed with the p-adic ultrametric. Its infinite branches are points of the ring ***Z_p***; in fact, ***Z_p*** coincides the unit ball**.** Thus, w.r.t. the hierarchic p-metric *the Universe, is bounded.* Topologically the p-adic universe differs crucially from the Universe endowed with the Euclidean or Minkowski geometry. The basic properties of ***Z_p*** match very well with the Bohm's views on implicate order. This space *is disordered, zero dimensional, and totally disconnected.*

4. From ontic (implicate) to epistemic (explicate)

In section 3, the mathematical structure of the ontic Universe was approached from the special dendrogram representation of experimental data. Now, we proceed another way around: from the ontic p-adic model to the epistemic dendrogramic model. Our previous epistemic-to-ontic pathway (section 3) centralized the role of an observer *O*. This can make the

Preprints (www.preprints.org) | NOT PEER-REVIEWED | Posted: 14 June 2021 doi:10.20944/preprints202106.0369.v1

impression that the personal observer perspective plays the crucial role in DH-theory (cf. with QBism [45]). Now, by starting with p-adic ontic model we diminish subjective component.

The points of the p-adic tree ***Z_p*** represent all possible events which can happen in the Universe. Thus, as well as the epistemic Universe, the ontic Universe is represented as a set of events. However, these are not observational events; they cannot be associated with say the clicks of detectors. We consider the p-adic points, *absolute events*. An absolute event is the endpoint of the infinitely long path of the p-adic tree, mathematically a sequence

$$a=a1....an ...., \text{ with coordinates } aj=0,1,..., p-1.$$

Each finite cutoff of the infinite path *a* is an element of the explicate order, it can be interpreted as the characteristic of a physical system. The latter is determined in a variety of ways depending on the embedding of the finite path *a'=a1....an* into various dendrograms. We consider the following process of structuring of the ***Z_p*** -universe. Let us select some set of points *S* of ***Z_p*** (finite or infinite), these points are geometrically presented as paths starting at the root of the p-adic tree. Thus, *S* is a subtree of this tree. The common roots of these paths determine relational closeness of corresponding points in *S*. As well as in the epistemic model, these points can be considered as characteristics of *S.* Observer is not involved in this consideration. Roughly speaking the system *S* exists irrespectively whether somebody looks at it or not.

Now take the tree of an ontic system *S* and cut it at some level, say *n* steps from the root. Such dendrogram expresses a system *S_n* belonging to the explicate level of nature's description. In principle, there is no need to couple it to some observer. This construction provides the realist interpretation even for systems represented by finite dendrograms. The only subjective element is the place of cutoff (cf. with the problem of boundary between quantum and classical world's).

Preprints (www.preprints.org) | NOT PEER-REVIEWED | Posted: 14 June 2021 doi:10.20944/preprints202106.0369.v1

5. The role of clustering algorithm

Different hierarchic clustering algorithms generate different dendrograms and observer's free will also covers algorithm's choice. However, in the ontic description this dependence on the algorithm's choice is washed out. All algorithms with p-alternatives branching generate approximations for the same ontic model of the Universe, given by the *p*-adic tree. The rings of *p*-adic numbers $\boldsymbol{Z_p}$ are not isomorphic for different *p*. However, their topological and algebraic properties are the same. Similar problem had been discussed in p-adic theoretical physics [19-28]: What *p* does correspond to the physical reality? There were various suggestions, including such exotic choices as *p=127* [26]. The pragmatic solution was to treat all *p*-adic models on the equal grounds and consider the *p*-adic encoding similarly to representation of real numbers by using different bases.

Of course, there exist clustering algorithms which generate nonhomogeneous trees, with different branching indexes for different vertexes. Such dendrogramic models lead to arbitrary trees (arbitrary ultrametric spaces). One may try to exclude such models by appealing to relational scale homogeneity of nature. In any event, we keep to p-adic models. Our original choice of the concrete hierarchic clustering algorithm [1] was motivated by studies including data-analysis of Murtagh [46-48]. In the present paper, we played with a few other algorithms, but their outputs are very similar with slight difference in details. In the following result section (section 11.3) we have applied seven different linkage clustering algorithms with no apparent differences in CHSH values outcomes (Figure 5 at section 11.3). We refer the interested reader to the matlab software web-site for details on those seven linkage clustering algorithms [49].

6. ``Traditional p-adic theoretical physics'': emphasis of the number-theoretic structure

We recall that on *p*-adic trees, it is possible to introduce arithmetic operations; algebraically these spaces are similar to the real line. However, topologically p-adic trees differ crucially from the real line. *P*-adic theoretical physics (see, e.g., [19-28] and references herein) floured in 1990s stimulated

Preprints (www.preprints.org) | NOT PEER-REVIEWED | Posted: 14 June 2021 doi:10.20944/preprints202106.0369.v1

by string theory [19, 21,22]. Its main problem which finally led to essential damping of its development during the recent years was the absence of coupling with the real experimental data. Roughly speaking there are no measurement devices generating *p*-adic outputs. But, as was clearly stated by Volovich [26], there are neither measurement devices generating irrational numbers, due to the finite precision of measurements all their outputs are rational numbers. Volovich claimed that the only physical numbers are the rational numbers. Since rational numbers are dense both in real and p-adic fields, he suggested unification of standard and p-adic physics on the basic of rational numbers. Although he did not use the ontic-epistemic terminology, we can say that for him mathematically epistemology is based on rational numbers, beyond this general rational epistemology one can recover the real and p-adic ontic models. We suggest another epistemology for p-adic ontology. This is the hierarchic relational epistemology. It differs crucially from the real-order epistemology of "standard physics". We can say Volovich's approach was number theoretical and our approach is hierarchic relational.

The DH-framework provides the rigid coupling of theory and experimental data. We hope that it will lead to the renaissance of p-adic modelling in physics. (We guess that its main theoretical results can be adapted to DH-theory.)

7. Dendrogram viewpoint onto classical-quantum interrelation

In our epistemic model, the sharp classical-quantum separation disappears. *The degree of classically is based on system's complexity* – the size and topological complexity of its dendrogram representation. Quantum systems are characterized by low complexity of their dendrograms. So, electrons and atoms can behave quantum in some measurements, because they have very simple hierarchic structure of interrelation between their components. In our approach, not only systems described by quantum mechanics, but even classical physical systems can exhibit quantum(-like) behavior within hierarchic representation of experimental data.

Preprints (www.preprints.org) | NOT PEER-REVIEWED | Posted: 14 June 2021 doi:10.20944/preprints202106.0369.v1

How can one measure the degree of ``quantumness''? In quantum physics, one of the most important tests is based on the CHSH inequality and other Bell type inequalities [50-55]. We select four system's characteristics (the end points of dendrograms representing systems) *a,a',b,b'* and calculate the correlations for pairs *(a,b), (a,b'), (a',b), (a',b').* Finally, CHSH-combination of correlations is formed and problem of its exceeding of two is studied via numerical simulation. For Alice and Bob, there are fixed settings *a, a'* and *b, b'*, respectively. Experimenter calculates the correlations Cab, Cab', Ca'b, Ca'b' and then the CHSH-combination of them:

C=Cab - Cab'+Ca'b+Ca'b'

Inequality |C| >2 means data collected in experimental runs is consistent with predictions of quantum theory and contradict to local legalism, i.e., it cannot be described by hidden variables model which is local.

We consider two time series of experimental data. Data is collected in measurements of one fixed classical physical observable. The outcomes of this observable carry the information about hierarchic relations between characteristics of a physical system under measurement. (Data is decomposed in the systems by the observer.) These relations are not visible in the straightforward graphic representation of data (see Fig.1). They are extracted from `` real data'' with the aid of clustering algorithm.

The standard viewpoint on violation of the Bell type inequalities [50-55] is that it shows that *"Quantum correlations are stronger than classical ones."*

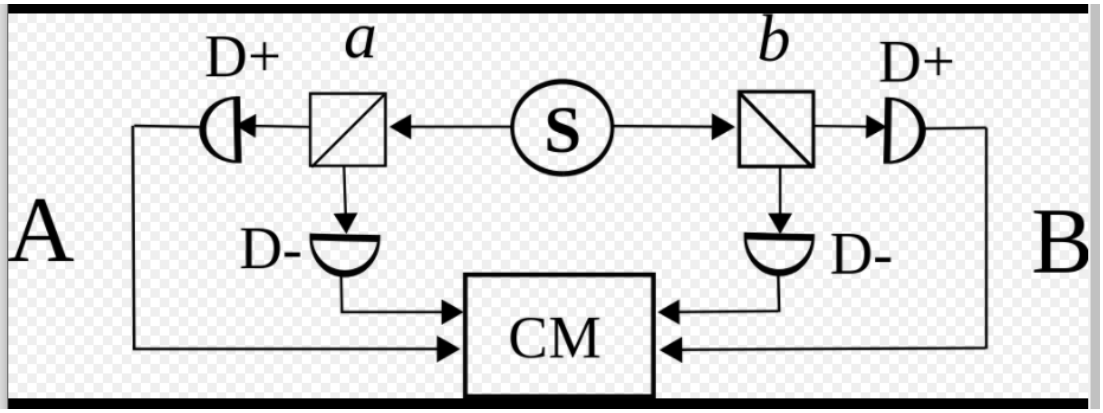

By

Preprints (www.preprints.org) | NOT PEER-REVIEWED | Posted: 14 June 2021 doi:10.20944/preprints202106.0369.v1

illustration 2. The scheme of the CHSH-test for two fixed settings *a* and *b* of polarization beam splitters.

By trying to explain this difference between quantum and classical correelations, Bell and his followers pointed to contradiction between quantum theory and local realism. The latter is mathematically formalized as representation of observables by functions of hidden variables; locality means that say Alice's functions do not depend on settings selected for Bob's functions, i.e., Sa=Sa (u), where u is the hidden variable.

The interpretation of the violation of the Bell inequalities is the subject of hot foundational debates (see, e.g., [56-60]). A plenty of so called loopholes were pointed out. Two basics of them, the nonlocality and detection efficiency loopholes [61, 62], were successfully closed in 2015-experiments [63-66].

8. The role of nonergodicity

De Broglie [67] was the first who highlighted that the experimentally obtained probabilities may deviate from ontic probability distribution of hidden variables. He justified this possibility within his double solution theory – in terms of the pilot wave. It seems that Krennikov's works [68-70] were the first publications in which there was pointed out to the difference between the frequency experimental probabilities and the measure-theoretic distributions of hidden variables. Khrennikov appealed to the von Mises' frequency probability theory. The latter straightforwardly implied that the Bell type inequalities can be violated for local models. However, it seems to be impossible to formalize mathematically the notion of realism within the von Mises frequency theory [71]. Finally, in [37] the interplay between frequency and measure-theoretic probabilities was structured within *ergodic theory* and it was shown that the violation of ergodicity is a sufficient condition for the violation of the Bell type inequalities. However, this was shown in the purely theoretical framework. In our further considerations, we shall show that in DH-theory the Bell inequalities are violated because of nonergodicity of time series of experimental data restructured with hierarchic clustering algorithms,

Preprints (www.preprints.org) | NOT PEER-REVIEWED | Posted: 14 June 2021 doi:10.20944/preprints202106.0369.v1

Hence, in DH-theory the Bell type inequalities are not the tool for rejection of the local realistic description or classical probability model (Kolmogorov [72], 1933). For our purpose, it is more natural to treat these inequalities as expressing the degree of quantumness of experimental statistical data – in the spirit of article [73].

As was mentioned in introduction, a few authors pointed out that quantum effects can be derived in classical statistical framework by rejecting the assumption of ergodicity [34-38]. In particular, in [35] it was guessed that the originally so emphasized the difference between quantum and classical statistical modeling can be eliminated by rejecting the hypothesis of ergodicity of data; even the black body radiation can be modelled classically, but within nonergodic statistical mechanics. In paper [37], *nonergodicity was pointed as one of the sufficient conditions for violation of the Bell type inequalities*, the condition which is equally important as nonlocality and rejection of realism (the hidden variables description).

DH-theory gives the possibility to introduce hidden variables (of the special type) beyond any experimental data and consider a class of realistic observables, those represented as functions of hidden variables. Hence, straightforwardly it seems that Bell type inequalities cannot be violated under the assumption of locality. However, we show the violation of the CHSH inequality for special selection of ``settings'' determining the observables. The reason for this is precisely the violation of ergodicity, the measure-theoretic and frequency averages do not coincide [37].

However, the natural question arises: Why do the hierarchically determined observables violate the assumption of ergodicity? The answer for the question is that the hierarchical sub-systems have already encoded in them the hierarchical structure of the "universal" dendrogram as was demonstrated in our paper [1].

We shall directly check the hypothesis of ergodicity in section 10 and we shall show that for wide range of "settings'' the hierarchic observables are not ergodic. However, we also found that for some "settings" the observables are ergodic, but, nevertheless, the CHSH inequality is violated. How can it happen? This situation was also discussed in paper [37]:

Preprints (www.preprints.org) | NOT PEER-REVIEWED | Posted: 14 June 2021 doi:10.20944/preprints202106.0369.v1

"Consider two stationary ergodic processes x(t) and y(t). Is the vector process z(t) = (x(t), y(t)) ergodic? The answer is 'no'. We remark that this implies that the product x(t)y(t) of two ergodic processes need not be ergodic. Thus, in principle in quantum theory nonergodicity can be generated by measurements on compound systems. At the same time measurements of each system separately generate ergodic stationary processes. In such a case measurement on compound systems really have the special feature, nonergodicity."

And we really found that in the case of the violation of the CHSH inequality the product of Alice and Bob observables is always nonergodic.

9. Scheme for calculation of dendrogramic correlations

For concreteness, we consider $p = 2$.

Step 1. *From data time-series to dendrogram: hierarchic clustering of data.*

Consider a time series of some data *Z1 Z2 .. .Zn...*Split it into blocks of the length *d.* (On Fig. 1, these are blocks of the length 5). For each block, we construct (with hierarchic clustering algorithm) dendrogram having *d* basepoints. We obtain dendrogram time-series: $D_1,\ldots,D_s\ldots,$ All dendrograms have *k* levels, where $2^{k-1} < d \leq 2^k$. (For Fig. 1 A, $d = 5$, hence $k = 3$.)

Step 2. *From dendrogram time-series to 2-adic time series.*

First we remark that each dendrogram *D* can be represented by vectors of the form $(\alpha 0,\alpha 1,\ldots\alpha k)$, where $\alpha j = 0,1$. Each vector encodes a path on *D* from its root to the corresponding endpoint; *D* is selection of *d* vectors from 2^k vectors.

From this vector-representations, we move to representations by natural numbers, which we define as features of the dendrogram, by using the formula

$$(\alpha_0\alpha_1\ldots\alpha_k) = \alpha_0 + \alpha_1 2 + \alpha_2 2^2 + \ldots + \alpha_k 2^k.$$

Thus, from a series of dendrograms $D_1,\ldots,D_s\ldots,$ we obtain a series of natural numbers, which are sorted in an ascending order, in each block of length d, according to the hierarchical structure of each dendrogram Dn,

Preprints (www.preprints.org) | NOT PEER-REVIEWED | Posted: 14 June 2021 doi:10.20944/preprints202106.0369.v1

These natural numbers play the role of polarization in the real CHSH experiment. Later we shall define new observables depending on such analogs of polarization. These d-blocks of natural numbers can be treated as hidden variables. New observables will be functions of these "hierarchic hidden variables".

Now, for correlations, we consider two time series $Z1\ Z2\ ..\ .Zn...$ and $Z1'\ Z2'\ ...\ .Zn'...$ and by applying the procedures of Steps 1,2, we obtain two series of dendrograms $D_1,....,D_s...$ and $D'_1,....,D'_s....$, and two corresponding series of natural numbers. They are formed from consecutive blocks of d natural numbers which are generated through d-decomposition of original time series:

$x=x_1x_2....x_n,\ \ x_n$ *is composed of blocks with d natural numbers*

$y=y_1y_2....y_n,\ \ y_n$ *is composed of blocks with d natural numbers*

Step 3. Defining of observables.

First method

We constructed two time series of dendrogram one for **Alice A=(A1A2A3…An)** and one for **Bob B=(B1B2B3…Bn)**.

For **Alice** we select two pairs of numbers **a**=[a1 a2] **a'**=[a1' a2'] the two pairs aren't identical. Analogs of two vectors – orientations of polarization beam splitters or Stern-Gerlach magnets.

For **Bob** we select two pairs of numbers **b**=[b1 b2] **b'**=[b1' b2'] the two pairs aren't identical.

For each Ai i∈1,2,3…n we randomly decided between pair a or a'

For each Bi i∈1,2,3…n we randomly decided between pair b or b'

If for **A**i we chose pair **a** we have the following:

If **A**i had both of the numbers in **a** we give Sai=1 else Sai=-1.

Metaphorically we can say that if "polarization" of **A**i coincides with a, the detector with the output is +1 clicks, if not, the detector with the output is -1 clicks.

We proceed in the same for selection of a' and b, b'. Then we calculate the correlations:

Preprints (www.preprints.org) | NOT PEER-REVIEWED | Posted: 14 June 2021 doi:10.20944/preprints202106.0369.v1

Cab=(∑Sai*Sbi)/ length(a and b are selected together)

Cab'=(∑Sai*Sb'i)/ length(a and b' are selected together)

Ca'b=(∑Sa'i*Sbi)/ length(a' and b are selected together)

Ca'b'=(∑Sa'i*Sb'i)/ length(a' and b' are selected together)

C=Cab - Cab'+Ca'b+Ca'b'

Second method

We constructed two time series of dendrogram one for **Alice A=(A1A2A3…An)** and one for **Bob B=(B1B2B3…Bn)**.

For **Alice** we select two pairs of numbers **a**=[a1 a2] **a'**=[a1' a2'] the two pairs aren't identical.

For **Bob** we select two pairs of numbers **b**=[b1 b2] **b'**=[b1' b2'] the two pairs aren't identical.

For each Ai i∈1,2,3…n we randomly decided between pair a or a'

If for **A**i we chose pair **a** we have the following

We replace the natural number in Ai that equal a1 to 1

We replace the natural number in Ai that equal a2 to -1

We replace all other natural numbers in Ai 0. we indicate that pair **a** was chosen to Ai .

The same we do for other settings, a', b, b'-

We find i that a and b were chosen = nab

We find i that a' and b were chosen = na'b

We find i that a and b' were chosen = nab'

We find i that a and b' were chosen = na'b'

We calculate Sab=(Ai=nab) *(Bi=nab)

We calculate Sa'b=(Ai=na'b) *(Bi=na'b)

We calculate Sab'=(Ai=nab') *(Bi=nab')

We calculate Sa'b'=(Ai=na'b') *(Bi=na'b')

Preprints (www.preprints.org) | NOT PEER-REVIEWED | Posted: 14 June 2021 doi:10.20944/preprints202106.0369.v1

For block j of size d of Sab if there are two values of 1 we assign Xabj=1,one value of 1 Xabj=1 ,one value of -1 Xabj=-1, all values 0 Xabj=-1.

For block j of size d of Sab if there are two values of 1 we assign Xa'bj=1,one value of 1 Xa'bj=1 ,one value of -1 Xa'bj=-1, all values 0 Xa'bj=-1.

For block j of size d of Sab if there are two values of 1 we assign Xab'j=1,one value of 1 Xab'j=1 ,one value of -1 Xab'j=-1, all values 0 Xab'j=-1.

For block j of size d of Sab if there are two values of 1 we assign Xabj=1,one value of 1 Xa'b'j=1 ,one value of -1 Xa'b'j=-1, all values 0 Xa'b'j=-1.

We calculate

Cab=(∑Xabj)/length(Xabj)

Cab'=(∑Xab'j)/length(Xab'j)

Ca'b=(∑ Xa'bj)/length(Xa'bj)

Ca'b'=(∑ Xa'b'j)/length(Xa'b'j);

C=Cab-Cab'+Ca'b+Ca'b'

10. Non-Ergodicity check methods

Nonergodicity means that measure-theoretic and frequency averages do not coincide. We cliam that this is the main reason for violation of the CHSH inequality. We have operated with the frequency averages
S_{ab} =< *Sa,Sb* >, but the standard proofs of the Bell type inequalities are done for measure-theoretic correlation $S_{ab,\text{measure}}$ =<< *Sa,Sb* >>. *In order to check whethear our data is ergodic we continue with first scheme*

10.1 Scheme for determining if Data is Non-Ergodic

We start with one sequence A = ($A1A2....An$), where each d-vector Aj = ($u1,u2,...,ud$) represents a dendrogram. We fix *a=[a1 a2]* and define

$$Sa = Sa(u), \qquad (1)$$

We continue to calculate *Sa as in the first method of step 3 in section 9*. We stress that (1) is the condition of realism, the value of hidden variable u determines the outcome of the observable *Sa.* Then

$$< Sa >= (\sum_{j=1}^{n} Sa(A_j))/N \qquad (2)$$

Preprints (www.preprints.org) | NOT PEER-REVIEWED | Posted: 14 June 2021 doi:10.20944/preprints202106.0369.v1

is the frequency average. Now we compute the probability distribution of hidden variables. Let us fix one d-vector u which is present in our dendrograms and calculate proportion
number of occurrences of u

$$p(u) = \frac{number\ of\ occurrences\ of\ u}{n} \qquad (3)$$

Then

$$\ll Sa \gg = \sum_u Sa(u)p(u) \qquad (4)$$

where the sum is w.r.t. all hidden variables u which are present in our sequence of dendrograms. In the simplest situation, we should get that

$<< Sa >> \neq < Sa >$

and the deviation should be visible, not just very small deviation.

10.2 Scheme for determining if correlations between Data are Non-Ergodic

However, it can be that at the level of one sequence the ergodicity holds, but it is violated for correlation (I have a paper about this possibility and it seems that violation of CHSH can be of this type).
Then, let us proceed without the random choice and calculate for $A = (A1...An), B = (B1...bN)$ *Sa and Sb as in the first method of step 3 in section 9*. Thus our frequency correlation:

$$< Sa, Sb >= (\sum_{j=1}^{n} Sa(A_j)Sb(B_j))/N \qquad (5)$$

Then we should complete this analysis by the measure-theoretic framework. We consider all possible pairs of hidden variables, d-vectors, u,v which are

Preprints (www.preprints.org) | NOT PEER-REVIEWED | Posted: 14 June 2021 doi:10.20944/preprints202106.0369.v1

present in the pairs *Aj,Bj* and find the probability number of occurrences of u,v

$$p(u,v) = \frac{number\ of\ occurrences\ of\ u,v}{n} \qquad (6).$$

And

$$\ll Sa,Sb \gg = \sum_{u} Sa(u)Sb(v)p(u,v) \qquad (4)$$

and for non-ergodic correlations we expect that

$<< Sa,Sb >> \neq < Sa,Sb >$

11. Results

In what follows we define the two distances metrics,

euclidean: $euclidean\ distance = \sqrt{(x_i - x_j)^2}$

were $x \in spatial\ data\ point,\ \ i,j \in 1,2 \ldots n.\ n = d\ block\ size$

and minkowski:

$$minkowski\ distance = -(t_i - t_j)^2 + (x_i - x_j)^2$$

Were $x \in spatial\ data\ point,\ \ i,j \in 1,2 \ldots n.\ n = d\ block\ size$

$t \in temporall\ data\ point, \qquad i,j \in 1,2 \ldots n.\ n = d\ block\ size$

We analyzed the same data sets by

applying section 9 Scheme (first and second method) for calculation of dendrogramic correlations for **three different "views"** of the data sets:

1. we constructed dendrograms with the euclidean distance metric which will be shown in section 1 of the results.
2. we constructed dendrograms with the minkowski distance metric which will be shown in section 2 of the results.
3. we Lorentz transformed the data sets and then constructed dendrograms with the minkowski distance metric

11.1 CHSH vaulations for 2-slit diffraction experiment data

Preprints (www.preprints.org) | NOT PEER-REVIEWED | Posted: 14 June 2021 doi:10.20944/preprints202106.0369.v1

As an example, we reproduced the Bell violations of correlations from a very classical double slit diffraction experiment [74] . the original experiment used a CCD camera with 512x512 detectors chip. The detection pattern in each frame in the experiment was represented as a binary matrix of 512x512 were 0 values represent no detection of photons in the corresponding detector while 1 value represented detection of photons in the corresponding detector . for each frame and its corresponding binary matrix we found all column positions that had the value 1, multiplied these positions value and calculated the log10 value of the outcome, this resulted in a unique number representing each frame detection pattern.

Thus, each frame was encoded with only one unique number A_f and time number T_f in which f∈frame 1 2..n. From each number of consecutive frames, N, the pairwise distances between each of the N A_f was calculated. Pair wise distances were calculated according to the above three views of the data sets data three methods: first by applying an euclidean distance metric between each A_f values , secondly, by applying minkowski distance metric between each two vectors [T_f A_f] and thirdly by applying Lorentz transformation on each vector [T_f A_f] where the reference frame was 0.99 the speed of light and then each Lorentzian transformed vector [T_f A_f]$_{lorentzian}$ was compared to another Lorentzian transformed vector by applying minkowski distance metric between such vectors.

Dendrogram were constructed by using ward or weighted linkage algorithm. The result was a series of consecutive denenrograms $D1D2...Dn$ with block length/edge number in single dendrogram d=4,5..9.

For each such d we splited the dendrogram series into two series of dendrograms each of length n/2. One series is the observable Alice measures And the second series is the observable Bob measures. As in step2 of section 9 we represented each dendrogram edge Dn with a natural number (feature). These features were sorted in an ascending order according to the hierarchical structure of the dendrogram. We then carried on to evaluate CHSH correlations in accordance to step 3 first and second method.

11.2 First method CHSH

In line with first method of step 3 in section 9 we calculated CHSH values for each combination of features ab=[[a b] [a b'] [a' b] [a' b']]

Where all a, a', b and b' are chosen out of the number of features in the whole 2 dendrogram series. Culumative distribution functions (cdf's) of CHSH values of all pair combination are shown in figure 1. Dandrograms were constructed with block size d=4,5..9 in three different ways corresponding to the 3 views described above. All views in all block sizes d=4,5..9 showed a

Preprints (www.preprints.org) | NOT PEER-REVIEWED | Posted: 14 June 2021 doi:10.20944/preprints202106.0369.v1

fraction of the pairs producing CHSH values above 2 resulting in the violation of CHSH inequality

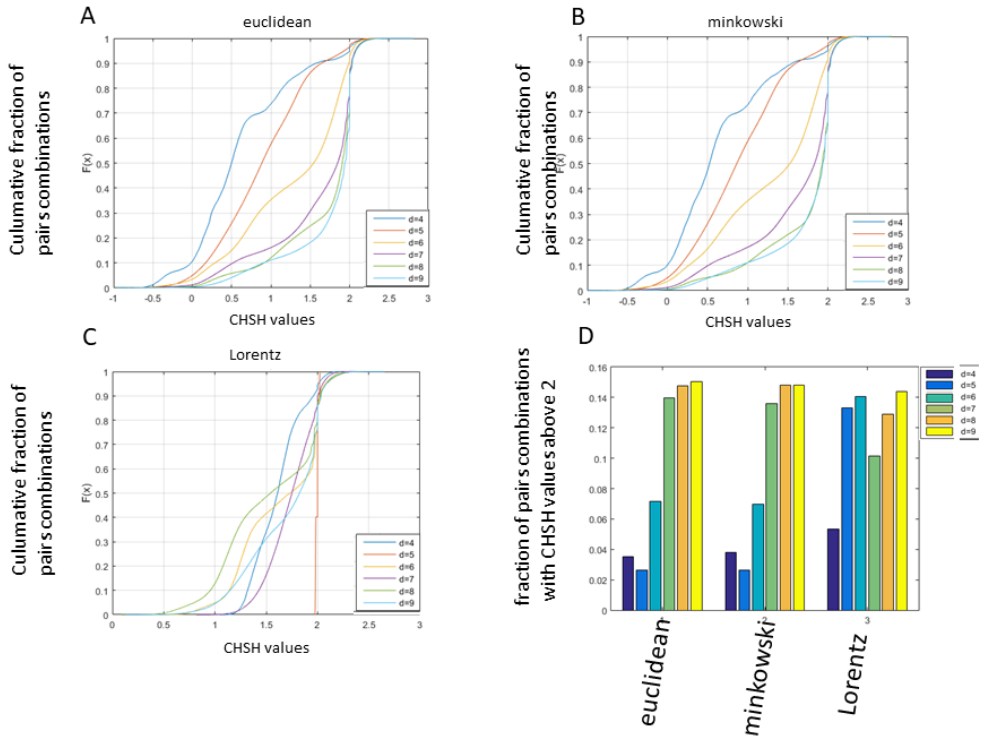

Figure 1: **CHSH values computed according to the first method in section 9 step 3.** (A) Cdf's of CHSH values with Euclidean view under "ward" linkage clustering algorithm. Each cdf corresponds to block size d=4,5..9. (B) Cdf's of CHSH values with Minkowski view under "ward" linkage clustering algorithm. Each cdf corresponds to block size d=4,5..9. (C) Cdf's of CHSH values with LOrentzian view under "ward" linkage clustering algorithm. Each cdf corresponds to block size d=4,5..9. (D) fraction of CHSH with values Above 2 in each view, Euclidean,Minkowski and Lorentzian, with block sizes d=4,5..9.

in order to verify that non ergodicity is the cause for violation of the CHSH inequality we tested the amount of ergodicity of the dendrogramic data that CHSH values were calculated from (figure 2). We tested the data for any pair of features a=[a1 a2] as described in the ***Scheme for determining if Data is Non-Ergodic of*** section 10.1. the results show that the dendrogramic data for dendrograms of block size d=5,6..9 the mean ergodicity score (|<Sa>-<<Sa>>|) show considerable fraction of all possible a=[a1 a2] pairs with non

Preprints (www.preprints.org) | NOT PEER-REVIEWED | Posted: 14 June 2021 doi:10.20944/preprints202106.0369.v1

zero value indicating clear Non-Ergodicity. Moreover cross-correlating the fraction of CHSH values above 2 and the data ergodicity score in each dendrogram of block size d=5,6..9 for the Eucliden metric view, Minkowski view and Lorentzian view resulted in correlation coefficients -0.9485, -0.9772 and -0.0025 respectively

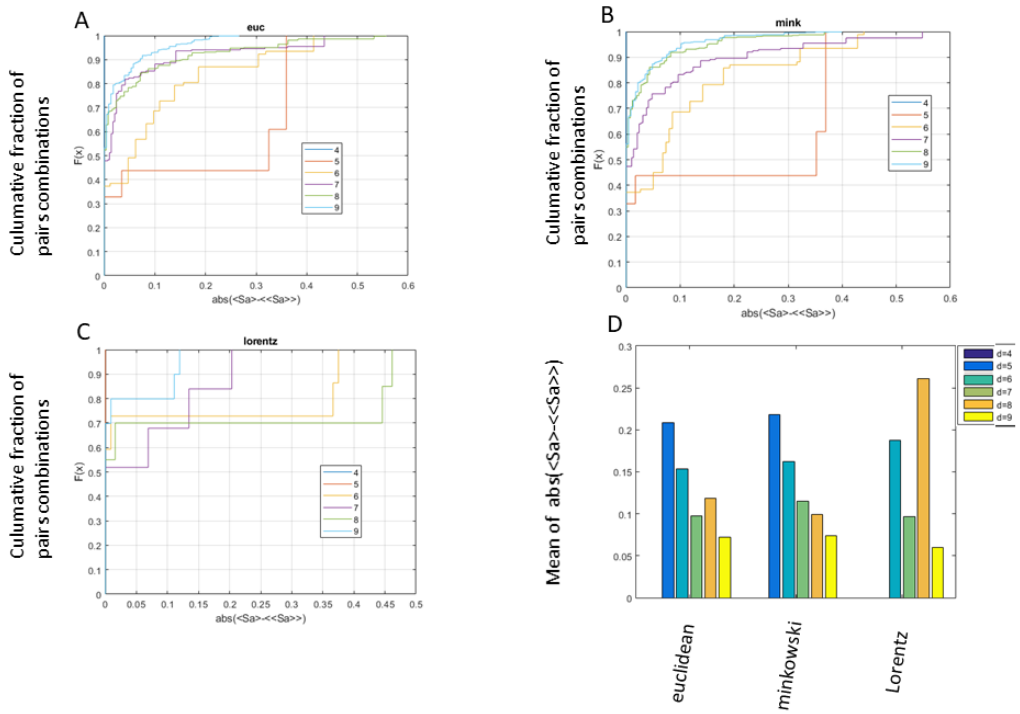

Figure 2: **Ergodicity score values computed according to the *Scheme for determining if Data is Non-Ergodic* described in section 10.1.** (A) Cdf's of Ergodicity score values with Euclidean view under "ward" linkage clustering algorithm. Each cdf corresponds to block size d=4,5..9. (B) Cdf's of Ergodicity score values with Minkowski view under "ward" linkage clustering algorithm. Each cdf corresponds to block size d=4,5..9. (C) Cdf's of Ergodicity score values with Lorentzian view under "ward" linkage clustering algorithm. Each cdf corresponds to block size d=4,5..9. (D) Mean of Ergodicity score in each view, Euclidean,Minkowski and Lorentzian, with block sizes d=4,5..9.

We note that for all views the dendrogram data series with block size d=4 showed the data is ergodic . thus the violation of CHSH inequality for block size d=4 can be a result of correlation non-ergodicity. We carried on to

Preprints (www.preprints.org) | NOT PEER-REVIEWED | Posted: 14 June 2021 doi:10.20944/preprints202106.0369.v1

investigate ergodicity in terms of two stationary ergodic series correlations in the Euclidean view. This ergodic test for correllations is described in the ***Scheme for determining if correlations between Data are Non-Ergodic*** in section 10.2. The results of this investigation clearly show all d=4,5..9 block size dendrograms are nonergodic, in terms of correlations, in the Euclidean view (figure 3).

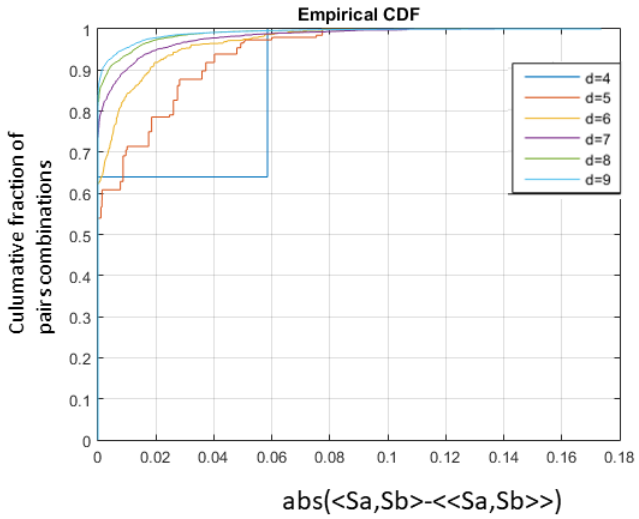

Figure 3: **Ergodicity score values computed according to the *Scheme for determining if correlations between Data are Non-Ergodic* described in section 10.2.** Cdf's of Ergodicity score values with Euclidean view under "ward" linkage clustering algorithm. Each cdf corresponds to block size d=4,5..9.

11.3 second method CHSH

In line with second method of step 3 in section 9 we calculated CHSH values for each combination of features *ab*=[[*a b*] [*a b'*] [*a' b*] [*a' b'*]]
Where all a, a', b and b' are chosen out of the number of features in the whole 2 dendrogram series. Culumative distribution functions (cdf's) of CHSH values of all pair combination are shown in figure 4. Dandrograms were

Preprints (www.preprints.org) | NOT PEER-REVIEWED | Posted: 14 June 2021 doi:10.20944/preprints202106.0369.v1

constructed with block size d=4,5..9 in three different ways corresponding to the 3 views described above. Again as with the first method All views in all block sizes d=4,5..9 showed a fraction of the pairs producing CHSH values above 2 resulting in the violation of CHSH inequality (figure 4). Interestingly the fraction of CHSH values above 2 in the Euclidean and minkowski views showed descending fraction values in respect to increasing d value d=4,5..9 in contrast to the first method which showed ascending relation with increasing d values.

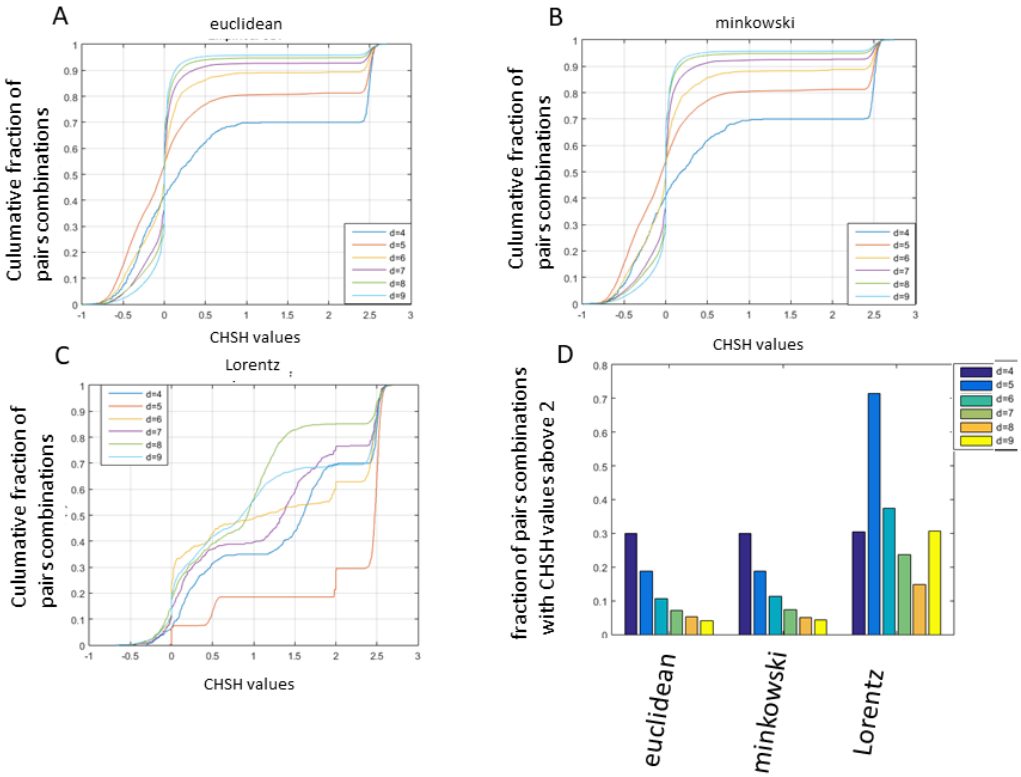

Figure 4: **CHSH values computed according to the second method in section 9 step 3.** (A) Cdf's of CHSH values with Euclidean view under "ward" linkage clustering algorithm. Each cdf corresponds to block size d=4,5..9. (B) Cdf's of CHSH values with Minkowski view under "ward" linkage clustering algorithm. Each cdf corresponds to block size d=4,5..9. (C) Cdf's of CHSH values with LOrentzian view under "ward" linkage clustering algorithm. Each cdf corresponds to block size d=4,5..9. (D) fraction of CHSH with values Above 2 in each view, Euclidean,Minkowski and Lorentzian, with block sizes d=4,5..9.

Preprints (www.preprints.org) | NOT PEER-REVIEWED | Posted: 14 June 2021 doi:10.20944/preprints202106.0369.v1

Please note that the Euclidean cdf's raise in correlation to the second ergodic test described in figure 3.
We further studied the dependance of the three views violation of CHSH inequlity on the linkage clustering algorithm (figure 5). For that purpose, we used 7 different algorithms all for d= 5 which showed no change in the Euclidean and minkowski views as to the fraction of pairs violating CHSH inequality. The Lorentz view showed a significant change in value in the "single" algorithm resulting in fraction of pairs value comparable to the Euclidean and Minkowski views.

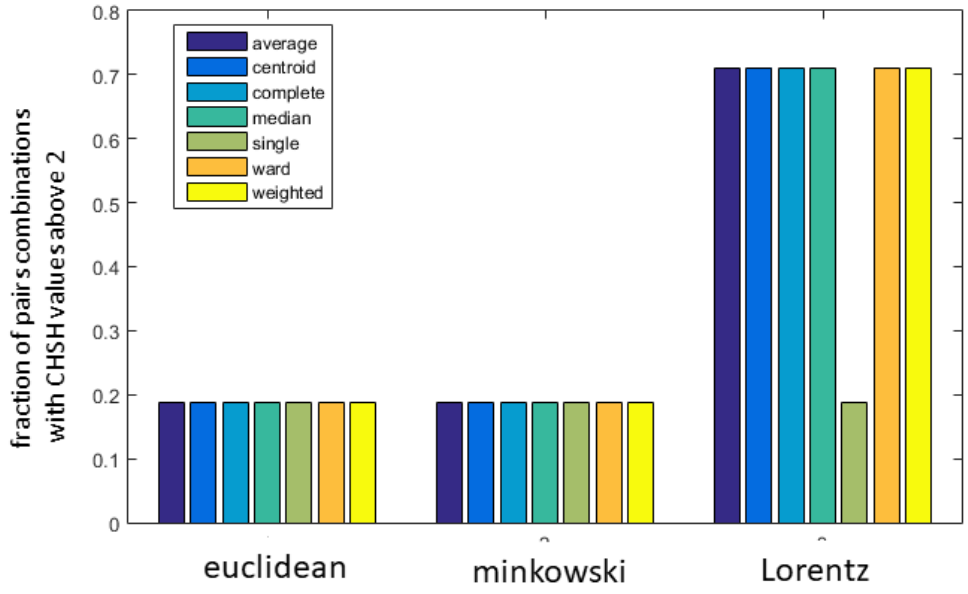

Figure 5: seven linkage clustering algorithms influence on CHSH inequality violation. fraction of CHSH with values Above 2 in each view, Euclidean,Minkowski and Lorentzian, with block sizes d=5 and in each of the 7 linkage clustering algorithms.

11.3.1 second method CHSH random data.

We carried on to produce 10 random numbers sequences (comparable in size of the number of frames in the 2-slit diffraction experiment) in order to compare the analysis to the diffraction 2-slits experiments correlation analysis.

Preprints (www.preprints.org) | NOT PEER-REVIEWED | Posted: 14 June 2021 doi:10.20944/preprints202106.0369.v1

For that purpose for each random number in one of the 10 sequences we used this scheme:
First we randomly choose a number between 1-7 which will indicate the amount of random numbers generated from the interval [1 512] (this is in correspondence to the 2-slit diffraction experiment with 512 detectors.
We multiplied these numbers and calculated the log10 value of the outcome, this resulted is a unique number representing each "randomly generated frame detection pattern". each such frame was accompanied with a time stamp which indicated the time of generation of the "randomly generated frame detection pattern". We carried to analyze, in each of the "views" as defined in section 10 above , the fraction of ab pairs that violated CHSH inequality. Mean fraction values of ab pairs, of ten random sequences, violating the CHSH inequality is shown in figure 6.

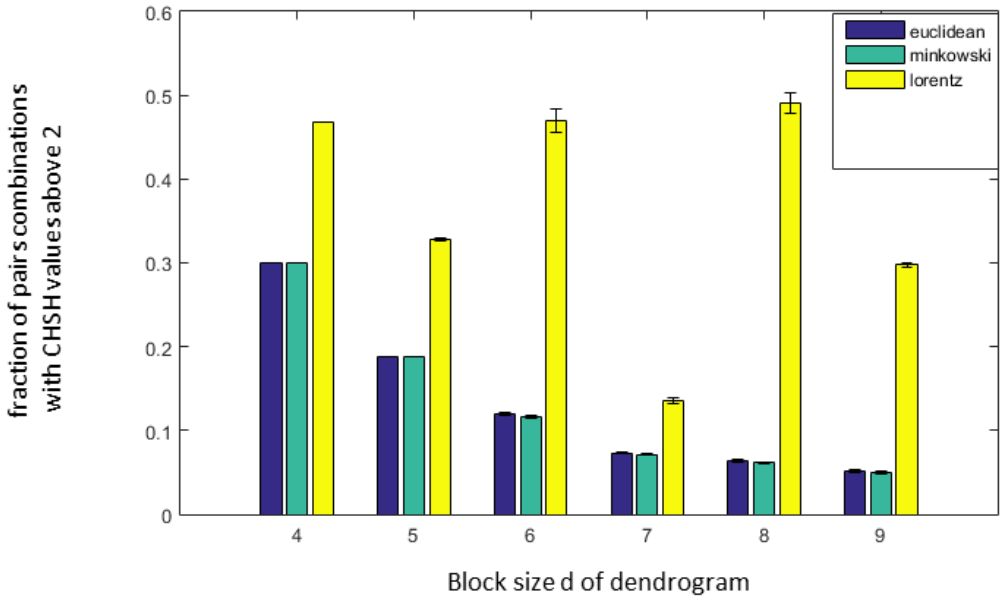

Figure 6: **Mean CHSH values computed from 10 sequances of random data according to the second method in section 9 step 3.**
fraction of CHSH with values Above 2 in each view, Euclidean,Minkowski and Lorentzian, with block sizes d=4,5..9 and in each with "ward" linkage clustering algorithm.

Preprints (www.preprints.org) | NOT PEER-REVIEWED | Posted: 14 June 2021 doi:10.20944/preprints202106.0369.v1

11.4 Lorentz transformed data.

As was clearly indicated by all the above analysis the Lorentz transformed data result in higher fraction of pairs violating the CHSH inequality under most of the clustering algorithms (although the "single" algorithm showed comparable CHSH fraction values , figure 5). One might wonder why. The explanation for that phenomena is that most clustering algorithms , except the "single" algorithm, produce dendrogram series with much smaller phase space of possible topology of dendrograms. This is clearly seen in figure 7 where we show the amount of features contained in the dendrogram series of the 10 random data sequences under each of the 3 views. The amount of features in the Lorentzian view remains small for all d=4,5..9.

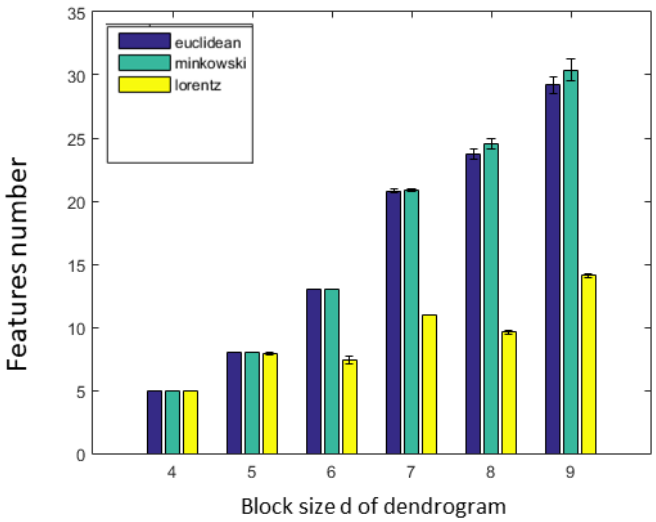

Figure 7: Mean feature number computed from 10 sequances of dendrogram composed out of random data . Mean feature number of 10 sequences in each view, Euclidean, Minkowski ans Lorentzian and in block size d=4,5..9.

12. Discussion on the results of numerical data analysis

We emphasize, our basic idea, that quantum-likeness is not the property of systems but of time series of observations. In the same way as randomness, quantum-likeness can be established on the basis of tests for data. For the moment, we considered only one (but very important) test, CHSH-test. Our main results are that

Preprints (www.preprints.org) | NOT PEER-REVIEWED | Posted: 14 June 2021 doi:10.20944/preprints202106.0369.v1

a) Violation of the CHSH inequality can be demonstrated by time series generated by measurements on classical systems.
b). The key-point is hierarchic dendrogramic representation of data. It can be described by local hidden variable model.
c). CHSH-violation is closely correlated with violation of ergodicity

Generally *nonergodicity is the fundamental property of hierarchic dendrogramic representation of statistical data.*

This representation is based on the application of clustering algorithms. Although different algorithms can generate different dendrogramic series, from the same experimental data, general properties of representations do not differ; all algorithms show CHSH-violation and nonergodicity of data or of correlations . Of course, the degree of violation and nonergodicity vary with algorithms (see figures 1,2,3,4 and 6).

By taking into account the temporal component of data-series, we generate two dimensional geometry endowed with Minskovski pseudo-metric. We apply DH-theory to this geometry. It was found that the basic properties of Minskovski DH-theory do not differ from its Euclidean version (figures 1,2,3,4 and 6). As the last step of our playing with algorithms, we performed Lorentz transformation of data and then proceed with dendrogramic modeling. Again, the Lorentz transformed data showed CHSH violations and nonergodicity of data (figure 1,2,3,4,5) although not with comparable values to the Euclidean and Minkowski views. We showed that these CHSH violations can become comparable with the violations under the Euclidean and Minkowski views under certain clustering algorithms (figure 5, “single” clustering algorithm). We also show that the high fraction of pairs showing CHSH violations in the Lorentzian view is a consequence of the smaller phase space of possible topology of dendrograms under most clustering algorithms which result in smaller amount of features (figure 7).

The two methods in step 3 of section 9 are different in the treatment of the hierarchical information of the data and adaptation to the formalization of the CHSH experiment in terms the hierarchical information. This different adaptation leads to some what different results where CHSH violations seem to be with opposite phase with d block size. Although this still needs to be investigated, we note that both methods show CHSH violations.

Preprints (www.preprints.org) | NOT PEER-REVIEWED | Posted: 14 June 2021 doi:10.20944/preprints202106.0369.v1

Some more simulations should be considered with d block size of larger size the nine in order to again verify the transition from quantum to classical correlations already discussed in previous study [1].

13. Concluding remarks

In this paper DH-theory [1] was structured in the ontic-epistemic (implicate-explicate order) framework. Experimental data is described by dendrograms generated by clustering algorithms – epistemic counterpart of our theory. In the limit dendrograms generate the infinite *p*-adic tree – the mathematical model of the ontic Universe.

DH-theory is realistic, not only because the epistemic theory of observations has the ontic background, but also because even at the epistemic level it is possible to introduce hidden variables. Ontic realism is very exotic: *The Universe zero-dimensional, totally disconnected and disordered.* This universe is bounded, but w.r.t. the very special distance, *p*-adic ultrametric. But maybe it is even more surprising that the local realistic description can be used event at the epistemic level, with hierarchic hidden variables and observables which their functions.

DH-theory provides a novel viewpoint on classical-quantum interrelation. First, we stress that the ontic *p*-adic world is classical. In the epistemic dendrogramic world simpler dendrograms have higher degree of quantum-likeness. For the moment, the latter is characterized with just one test of quantumness – the CHSH test. Its violation is a consequence of nonergodicity of empiric data. However, it is crucial that this data is represented dendrogramically.

Finally, we remark that the size of base-level of a dendrogram can be considered as system's dimension. It is interesting that we are able to violate the CHSH inequality only for d> 3.

Acknowledgments

Igor Volovich, Vladimir Anashin, Evgenii Zelenov, Varda and Boaz Dotan; Masha Shor.

Appendix A: Ultrametric spaces, trees, p-adic numbers

Preprints (www.preprints.org) | NOT PEER-REVIEWED | Posted: 14 June 2021 doi:10.20944/preprints202106.0369.v1

In some applications the point structure of a set X and the properties of a metric ρ may essentially differ from the Euclidean case. We are interested in metric spaces X where, instead of the standard triangle inequality, the strong triangle inequality:

$$\rho(x, y) \leq max[\rho(x, z), \rho(z, y)] \quad (1)$$

is valid. Such a metric is called an ultrametric, and such metric spaces are called ultrametric spaces. The strong triangle inequality can be stated geometrically: all triangles are isosceles.

Let us discuss the main properties of ultrametric space X. We set

$$B_r(a) = \{x \in X : \rho(x - a) < r\}, B_r \sim (a) = \{x \in X: \rho(x - a) \leq r\}, r > 0, a \in X$$

These are balls of the radius r with the center at the point a. Our standard intuition tells us that $B_r(a)$ is a closed ball, but not open, and $B_r \sim (a)$ is an open ball, but not closed. However, it is not valid for ultrametric spaces:

In ultrametric space each ball in X is open and closed at the same time. Each point of a ball may serve as a centre. A ball may have infinitely many radii.

Let U and V be two balls in ultrametric space X. Then there are only two possibilities: (1) balls are ordered by inclusion (i.e., $U \subset V$ or $V \subset U$); (2) balls are disjoint.

Thus if two balls have a common point then one has to be a part of another.

The symbol $S_r(a)$ denotes the sphere $\{x \in X: \rho(x, a) = r\}$ of the radius $r > 0$ with the center at a. There is also a large deviation from the Euclidean case: the sphere $S_r(a)$ is not a boundary of $B_r(a)$ or $B_r \sim (a)$.

Consider the following class of ultrametric spaces (X, ρ). Every point x has an infinite number of coordinates $x = (a_o, a_1, ..., a_n, ...)$. Each coordinate yields the finite number of values $a \in \{0, ..., m - 1\}$, where $p > 1$ is a natural number. We denote the space of sequences (1) by the symbol $X = \mathbf{Z_p}$. The standard ultrametric is introduced on this set in the following way.

Let $x = (a_0, a_1, a_2, ..., a_n, ...), y = (b_0, b_1, b_2, ..., b_n, ...) \in \mathbf{Z_p}$. We set

$$r\_p(x, y) = 1/m^k$$

$$\text{if } a_j = b_j, j = 0, 1, ..., k - 1, \text{ and } a_k \neq b_k \quad (3)$$

This is a metric and even an ultrametric. To find the distance $r\_p(x, y)$ between two strings of digits x and y, we have to find the first position k at which the strings have different digits. The space $X = Z_m$ coincides with the unit ball centered in zero, $X = B_1(0)$; this space is compact. Geometrically it can be represented by the tree, see Figure 8 for the 2-adic tree

Preprints (www.preprints.org) | NOT PEER-REVIEWED | Posted: 14 June 2021 doi:10.20944/preprints202106.0369.v1

representing $\mathbf{Z}_2$. Here one vertex, the root labeled as R, is incident for two edges and other vertices are incident for three edges. We remark that it is convenient to consider this tree as the directed graph; for each vertex I different from R, one edge comes from the branch starting at R, the "input edge", and two edges go out from I, the "output edges". These two edges (or vertices at their ends) are labeled by $a = 0, 1$. In Figure 8 the order of labeling of the output edges is based on the embedding of the tree in the plane, upper output edges are labeled by 0 and lower by 1. This leads to the concrete numerical representation of this tree. However, the rule used for labeling of edges is not obligatory; for each vertex I, we can assign 0/1 to each of output edges in an arbitrary way and obtain another numerical representation of this tree.

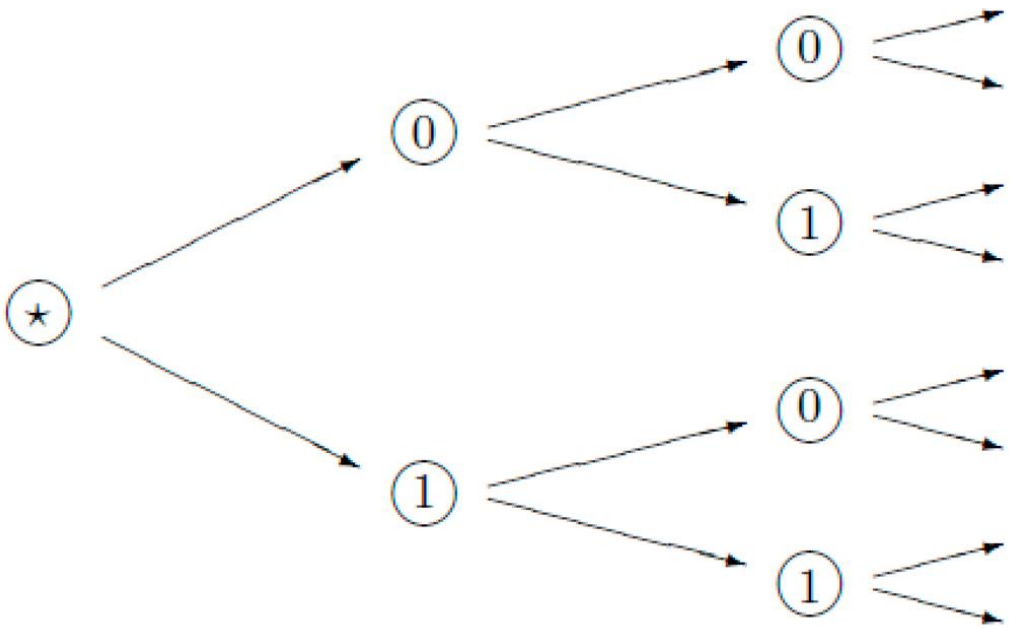

Figure 8: .2-adic hierarchic tree.

Appendix B: Clustering algorithms

A *linkage algorithm* computes the distance between two clusters.

The following notation describes the linkages used by the various methods:

- Cluster r is formed from clusters p and q.
- n_r is the number of objects in cluster r.
- x_{ri} is the ith object in cluster r.

Preprints (www.preprints.org) | NOT PEER-REVIEWED | Posted: 14 June 2021 doi:10.20944/preprints202106.0369.v1

- *Single linkage*, also called *nearest neighbor*, uses the smallest distance between objects in the two clusters.

$$d(r,s)=\min(dist(x_{ri},x_{sj})),i\in(i,...,n_r),j\in(1,...,n_s)$$

- *Complete linkage*, also called *farthest neighbor*, uses the largest distance between objects in the two clusters.

$$d(r,s)=\max(dist(x_{ri},x_{sj})),i\in(1,...,n_r),j\in(1,...,n_s)$$

- *Average linkage* uses the average distance between all pairs of objects in any two clusters.
- *Centroid linkage* uses the Euclidean distance between the centroids of the two clusters.
- *Median linkage* uses the Euclidean distance between weighted centroids of the two clusters.where $\tilde{x}_r$ and $\tilde{x}_s$ are weighted centroids for the clusters *r* and *s*. If cluster *r* was created by combining clusters *p* and *q*, $\tilde{x}_r$ is defined recursively as

$$\tilde{x}_r=0.5(\tilde{x}_p+\tilde{x}_q)$$

- *Ward's linkage* uses the incremental sum of squares, that is, the increase in the total within-cluster sum of squares as a result of joining two clusters. The within-cluster sum of squares is defined as the sum of the squares of the distances between all objects in the cluster and the centroid of the cluster.
- *Weighted average linkage* uses a recursive definition for the distance between two clusters. If cluster *r* was created by combining clusters *p* and *q*, the distance between *r* and another cluster *s* is defined as the average of the distance between *p* and *s* and the distance between *q* and *s*.

References

1. O. Shor, F. Benninger, A. Khrennikov, Representation of the universe as a dendrogramic hologram endowed with relational interpretation. *Entropy* **2021**, *23*(5), 584; https://doi.org/10.3390/e23050584.

2. Atmanspacher, H. Determinism is ontic, determinability is epistemic, in H. Atmanspacher and R.~C. Bishop (eds.), Between Chance and Choice: Interdisciplinary Perspectives on Determinism (Imprint Academic, Thorverton UK), 2002, pp. 49--74.

3 .Atmanspacher H., Primas H. (2003) Epistemic and Ontic Quantum Realities. In: Castell L., Ischebeck O. (eds) Time, Quantum and Information. Springer, Berlin, Heidelberg.

4. Hertz, H. (1899). The principles of mechanics: presented in a new form. London: Macmillan.

Preprints (www.preprints.org) | NOT PEER-REVIEWED | Posted: 14 June 2021 doi:10.20944/preprints202106.0369.v1

5. Boltzmann, L. (1905). Uber die Frage nach der objektiven Existenz der Vorgnge in der unbelebten Natur. In Barth, J.A. (Ed.) Populre Schriften: Leipzig.
6. Khrennikov, A. (2017). Quantum epistemology from subquantum ontology: Quantum mechanics from theory of classical random fields, Annals of Physics, 377, 147--163.
7. Khrennikov, A. Hertz's viewpoint on quantum theory. Act Nerv Super 61, 24 (2019). https://doi.org/10.1007/s41470-019-00052-1.
8. Brenner, J. E.; A. Igamberdiev, Philosophy in Reality; A New Book of Changes. Berlin-Heidelberg-New York, 2021.
9. David Bohm: *Wholeness and the Implicate Order*, Routledge, 1980
10. Khrennikov, A. Beyond quantum. Singapore: Pan Stanford Publ., 2014.
11. Jaeger, G. Quantum Objects: Non-Local Correlation, Causality and Objective Indefiniteness in the Quantum World; Springer: Berlin, Germany, New York, NY, USA, 2013.
12. Boughn, S. Making sense of Bell's theorem and quantum nonlocality. *Found. Phys.* **2017**, *47*, 640--657.
13. Fuchs, C.A. On Participatory Realism. In *Information and Interaction*; Springer: Berlin/Heidelberg, Germany, **2017**; pp. 113–134.
14. Smolin, L. *Einstein's Unfinished Revolution: The Search for What Lies beyond the Quantum*; Penguin Press: London, UK, 2019.
15. Cohen, E.; Cortês, M.; Elitzur, A.C.; Smolin, L. Realism and Causality II: Retrocausality in Energetic Causal Sets. *Phys. Rev. D* **2020**, *102*, 124028.
16. Cohen, E.; Cortês, M.; Elitzur, A.; Smolin, L.; Gan, R. Realism and causality I: Pilot wave and retrocausal models as possible facilitators. *Phys. Rev. D* **2020**, *102*.
17. Kupczynski, M. Closing the Door on Quantum Nonlocality. Entropy 2018, 20, 877.
18. Sciarretta, A. A local-realistic quantum mechanical model of spin and spin entanglement. Int. J. Quant. Inf. **2021**, *19*, No. 01, 2150006.
19. Volovich, I. p-adic string. *Cl ass. Quantum Gravity* **1987**, *4*, 83–87.
20. Vladimirov, V.S.; Volovich, I.V.; Zelenov, E.I. *p-Adic Analysis and Mathematical Physics*; World Scientific: Singapore, 1994.
21. Aref'eva, I.Y.; Dragovich, B.; Frampton, P.H.; Volovich, I.V. The wave function of the Universe andp-adic gravity. *Int. J. Mod. Phys. A* **1991**, *6*, 4341–4358. [CrossRef]
22. Freund, P.G.O.; Witten, E. Adelic string amplitudes. *Phys. Lett. B* **1987**, *199*, 191–194. [CrossRef]

Preprints (www.preprints.org) | NOT PEER-REVIEWED | Posted: 14 June 2021 doi:10.20944/preprints202106.0369.v1

23. Khrennikov, A. p-adic quantum mechanics with p-adic valued functions. *J. Math. Phys.* **1991**, *32*, 932–937. [CrossRef]
24. Khrennikov, A. *p-Adic Valued Distributions in Mathematical Physics*; Springer: Berlin/Heidelberg, Germany, 1994.
25. Parisi, G.; Sourlas, N. P-adic numbers and replica symmetry breaking. *Eur. Phys. J. B Condens. Matter Complex. Syst.* **2000**, *14*, 535–542. [CrossRef]
26. Volovich, I.V. Number theory as the ultimate physical theory. *P-Adic Numbers Ultrametric Anal. Appl.* **2010**, *2*, 77–87. [CrossRef]
27. Dragovich, B.; Khrennikov, A.Y.; Kozyrev, S.V.; Volovich, I.V.; Zelenov, E.I. P-adic mathematical physics: The first 30 years. *p-Adic Numbers Ultrametric Anal. Appl.* **2017**, *9*, 87–121. [CrossRef]
28. Anashin, V. Discreteness causes waves. Facta universitatis - series Physics Chemistry and Technology **2016,** *14*(3), 143-196
29. Bohr, N. Can quantum-mechanical description of physical reality be considered complete? *Phys. Rev. 1935*, 48,696-702.
30. N. Bohr, The quantum of action and the description of nature. In: Foundations of Quantum Physics I (1926–1932). Niels Bohr collected works. J. Kalckar (ed.), v. 6, Elsevier B.V., 1985, pp. 201-217.
31. Plotnitsky, A. Epistemology and Probability: Bohr, Heisenberg, Schrödinger and the Nature of Quantum-Theoretical Thinking}; Springer: Berlin, Germany; New York, NY, USA, 2009.
32. Plotnitsky, A. Niels Bohr and Complementarity: An Introduction; Springer: Berlin, Germany; New York, NY, USA, 2012.
33. Plotnitsky, A. "The Unavoidable Interaction Between the Object and the Measuring Instruments:" Reality, Probability, and Nonlocality in Quantum Physics. *Found Phys* 50, 1824–1858 (2020).
34. Buonomano, Quantum uncertainties, Recent and Future Ex-periments and Interpretations , edited by W.M. Honig, D.W.Kraft and E. Panarella, NATO ASI Series,162, Plenum Press,New York (1986)
35. Gallavotti, G. Ergodicity, ensembles, irreversibility in Boltzmann and beyond. *J. Stat. Phys.* **1995**, *78*, 1571–15.
36. A. Yu. Khrennikov, *p*-adic probability predictions of correlations between particles in the two slit and neuron interferometry experiments. *Il Nuovo Cimento* B **1998**, *113*, 751-760.
37. Khrennikov, A. Buonomano against Bell: Nonergodicity or nonlocality? Int. J. Quant. Inf. **2017**, *15*, No. 08, 1740010.
38. Hnilo, A. (2019). Beyond Loophole-Free Experiments: A Search for Nonergodicity. In O. Lombardi, S. Fortin, C. López, & F. Holik (Eds.),

Preprints (www.preprints.org) | NOT PEER-REVIEWED | Posted: 14 June 2021 doi:10.20944/preprints202106.0369.v1

Quantum Worlds: Perspectives on the Ontology of Quantum Mechanics (pp. 245-266). Cambridge: Cambridge University Press.

39. Barbour, J.; Smolin, L. Extremal variety as the foundation of a cosmological quantum theory. *arXiv* **1992**, arXiv:hep-th/9203041.
40. Barbour, J. Shape Dynamics. An Introduction. In *Quantum Field Theory and Gravity*; Springer: Basel, Switzerland, 2012.
41. Rovelli, C. Relational quantum mechanics. *Int. J. Theor. Phys.* **1996**, *35*, 1637–1678. [CrossRef]
42. Smolin, L. Quantum Mechanics and the Principle of Maximal Variety. *Found. Phys.* **2016**, *46*, 736–758. [CrossRef]
43. Cortês, M.; Smolin, L. The universe as a process of unique events. *Phys. Rev. D Part Fields Gravit. Cosmol.* **2014**, *90*, 1–30. [CrossRef]
44. Plotnitsky, A. Spooky predictions at a distance: reality, complementarity and contextuality in quantum theory. *Phil. Trans. R. Soc.* A **2019**, *377*, 20190089.
45. Fuchs, C.~A., Mermin, N.~D. and Schack, R. An Introduction to QBism with an Application to the Locality of Quantum Mechanics. *Am. J. Phys.* **2014**, *82*, 749-761.
46. Murtagh, F.; Contreras Albornoz, P. Algorithms for hierarchical clustering: An Overview. *Data Min. Knowl. Discov.* **2011**, *2*, 86–97. [CrossRef]
47. Murtagh, F. Ultrametric and Generalized Ultrametric in Computational Logic and in Data Analysis. *Horiz. Comput. Sci. Res.* **2011**, *2*.
48. Murtagh, F.; Contreras, P.; Downs, G. Hierarchical clustering of massive, high dimensional data sets by exploiting ultrametric embedding. *SIAM J. Sci. Comput.* **2008**, *30*, 707–730. [CrossRef]
49. https://www.mathworks.com/help/stats/linkage.html#mw_08b425f7-fc8c-480a-b618-f768817e8e11
50. Bell, J.S. On the Einstein-Podolsky-*Rosen paradox. Physics* **1964**, *1*, 195—200.
51. Bell, J.S. *Speakable and Unspeakable in Quantum Mechanics*, 2nd ed.; Cambridge University Press: Cambridge, UK, 2004.
52. Bell, J.S. On the problem of hidden variables in quantum theory. *Rev. Mod. Phys*. **1966**, *38*, 450-481.
53. Clauser, J.F.; Horne, M.A.; Shimony, A.; Holt, R.A. Proposed experiment to test local hidden-variable theories. *Phys. Rev. Lett.***1969**, *23*, 880.
54. Aspect, A. Experimental tests of Bell's inequalities in atomic physics, in Atomic Physics 8, Proceedings of the Eighth International Conference on Atomic Physics, edited by I. Lindgren, A. Rosen and S. Svanberg (1982).

Preprints (www.preprints.org) | NOT PEER-REVIEWED | Posted: 14 June 2021 doi:10.20944/preprints202106.0369.v1

55. Aspect, A. Bell's Theorem: The naive view of an experimentalist. quant-ph/0402001.
56. Khrennikov, A. (ed.) Quantum Theory: Reconsideration of Foundations, Växjö Univ. Press: Växjö, 2002.
57. Khrennikov, A. (ed) Foundations of Probability and Physics-2. Växjö Univ. Press: Växjö, 2003.
58. Adenier, G., Khrennikov, A. and Nieuwenhuizen, Th. M. (eds.) Quantum Theory: Reconsideration of Foundations-3, AIP, Melville, NY, *810*, 2006.
59. Adenier, G., Fuchs, C. and Khrennikov, A. (eds.) Foundations of Probability and Physics-3, AIP, Melville, NY, *889*, 2007.
60. Adenier, G., Khrennikov, A. Yu., Lahti, P., Manko, V. I., and Nieuwenhuizen, Th. M. (eds.) Quantum theory: reconsideration of foundations--4, AIP, Melville, NY, 962, 2008.
61. Aspect, A.; Dalibard, J.; Roger, G. Experimental test of Bell's Inequalities using time-varying analyzers. Phys. Rev. Lett. 1982, , 1804--1807.
62. G. Weihs et al., Violation of Bell's inequality under strict Einstein locality conditions. Phys. Rev. Lett. 81, 1998, S. 5039.
63. Hensen, B.; Bernien, H.; Dreau, A.E.; Reiserer, A.; Kalb, N.; Blok, M.S.; Ruitenberg, J.; Vermeulen, R.F.; Schouten, R.N.; Abellan, C.;~et~al. Experimental loophole-free violation of a Belli nequality using entangled
64. electron spins separated by 1.3 km. Nature 2015, 526, 682.
65. Giustina, M.; Versteegh, M.A.; Wengerowsky, S.; H.; steiner, J.; Hochrainer, A.; Phelan, K.; Steinlechner, F.; Kofler, J.; Larsson, J.Å; Abellan, C.;~et~al. A significant-loophole-free test of Bell's theo-rem with entangled photons. Phys. Rev. Lett. 2015, 115, 250401.
66. Shalm, L.K.; Meyer-Scott, E.; Christensen, B.G.; Bierhorst, P.; Wayne, M.A.; Stevens, M.J.; Gerrits, T.; Glancy, S.; Hamel, D.R.; Allman, M.S.;~et~al. A strong loophole-free test of local realism. Phys. Rev. Lett. 2015, 115, 2504.
67. De Broglie, L. The current interpretation of wave mechanics: a critical study. Elsevier, 1964.
68. Khrennikov, A.~Yu. *Interpretations of Probability* .VSP Int. Sc. Publishers, Utrecht/Tokyo, 1999; 2nd edítion, De Gruyter, Berlin, 2009.
69. Khrennikov, A. Einstein and Bell, von Mises and Kolmogorov: reality and locality, frequency and probability. *Found. Phys.* **2002** *32*, N. 7, 1159-1174, arXiv:quant-ph/0006016;
70. Khrennikov, A. (2009). Contextual Approach to Quantum Formalism, Springer, Berlin-Heidelberg-New York, 2009.

Preprints (www.preprints.org) | NOT PEER-REVIEWED | Posted: 14 June 2021 doi:10.20944/preprints202106.0369.v1

71. von Mises, R. The mathematical theory of probability and statistics. Academic, London, 1964.
72. Kolmolgoroff, A.~N. Grundbegriffe der Wahrscheinlichkeitsrechnung, Springer-Verlag, Berlin, 1933.
73. A. Khrennikov, Get rid of nonlocality from quantum physics. *Entropy* **2019**, *21*(8), 806.
74. Aspden, R. S. *et al.* Video recording true single-photon double-slit interference Video recording true single-photon double-slit interference. **671**, (2018).